

Surface Fluorination of Titanium Oxides and Applications

* Jae-Ho Kim¹⁾, Takashi Kimura²⁾, Susumu Yonezawa³⁾ and Masayuki Takashima⁴⁾

1), 2), 3), 4) *Department of Materials Science & Engineering, University of Fukui, Fukui 910-8507, Japan*

¹⁾ kim@matse.u-fukui.ac.jp

ABSTRACT

The dispersion stability and photocatalytic activity of TiO₂ particles were improved by the surface fluorination using fluorine gas (F₂) at a pressure less than 50.5 kPa at 25°C. Average particle sizes and zeta potentials of fluorinated TiO₂ (F-TiO₂) particles in all solvents were approximately 11 times smaller and 1.5 times larger, respectively, than those of untreated TiO₂ particles (2.5×10³ nm and -19 mV). In the photocatalytic activity of TiO₂, the UV-Vis absorption range of F3-TiO₂ with Ti³⁺ and Ti²⁺ valences expanded to about 500 nm. Also, the degradation ratio of methylene blue (73%) with F-TiO₂ was much higher than that (18%) with untreated TiO₂ at 4 h. However, TiOF₂ in F4-TiO₂ synthesized at 200°C severely affected the dispersion stability and the photocatalysis of TiO₂. To optimize the beneficial effects of surface fluorination considering the dispersion stability and photocatalytic activity, it is necessary to control the fluorine content (x), 0 < x < 0.5 in TiO_{2-x}F_{2x}.

1. INTRODUCTION

Nanosized TiO₂ is one of the most promising photocatalysts currently available. To achieve high activities in solution-phase catalysis, it is important to facilitate good dispersion of the catalyst. [1–3]. However, small particles tend to aggregate, resulting in low or complete absence of photocatalytic activity. Many studies have focused on the dispersion stability of TiO₂ particles in water [4–6]. Surface modification of TiO₂ nanoparticles is an effective method to minimize the agglomeration of TiO₂ particles [7–9]. Silane alkoxides with organic functional groups also have been widely used for this purpose. It is important to consider the high cost of surfactants required and the residues generated in the particles. Al₂O₃ and TiO₂ metal oxide particles tend to disperse in a highly polar solvent; in contrast, they tend to flocculate in a low dielectric solvent because the Hamaker constant between the particles is high in such a solvent [10, 11]. TiO₂ particles generally disperse well in water but not in other solutions such as acetone and ethanol. Many researchers have reported that the photocatalytic activity of TiO₂ can be improved using various fluorinating agents other than F₂ gas [12–14]. Park and Choi [15] reported that surface fluorination results in enhanced photocatalytic degradation of certain substrates because of the formation of electron trapping sites. Li et al. [16–18] attributed the enhanced photocatalytic activity of F-doped powders mainly

^{1), 3), 4)} Professor

²⁾ Graduate Student

to the creation of surface oxygen vacancies and the beneficial effects of F-doping. Yu et al. [19] also reported the incorporation of fluoride ions into a TiO₂ lattice using an NH₄F source. However, the surface fluorination of TiO₂ could have either a positive or negative effect depending on the fluorine contents in TiO₂ particles. The relationship between the photocatalytic activity and fluorine contents in TiO₂ using F₂ gas has not been reported. Our previous work proved that surface fluorination using F₂ gas is beneficial to the dispersion stability of TiO₂ particles in water [20]. F-TiO₂ particles with good dispersion stability were synthesized at a temperature lower than 100 °C using fluorine gas. The idea was to stabilize the TiO₂ particles by enabling their surfaces to carry an electric charge to create electrostatic repulsive forces that repel each other.

In this paper, we report the effects of surface fluorination on the dispersion stability of TiO₂ in various organic solvents and also investigate the relationship between fluorine contents in TiO₂ and the photocatalytic activity of TiO₂.

2. EXPERIMENTAL DETAILS

2.1 Preparation of fluorinated TiO₂ samples

TiO₂ particles (ST-21, anatase; 98% purity) were obtained from Ishihara Sangyou Kaisha, Ltd. Fluorine gas (99.5% purity) was supplied by Daikin Industries Ltd. Details of the fluorination apparatus have been given in our previous paper [21, 22]. Fluorinated TiO₂ (F-TiO₂) particles were prepared by direct fluorination using F₂ gas under various reaction conditions. Reaction temperature, fluorine pressure, and reaction time were set at 25–200 °C, 1–50 kPa, and 1 h, respectively.

2.2 Catalysts characterization

The structural and electronic properties of the samples were investigated using powder X-ray diffraction (XRD, XD-6100) and X-ray photoelectron spectroscopy (XPS, XPS-9010). The surface morphology of various samples was observed using a scanning electron microscope (SEM, s-2400; Hitachi Ltd.). The BET surface area was determined using a Micromeritics ASAP 2000 nitrogen adsorption apparatus.

2.3 Dispersion stability measurements

Particle size distribution and zeta potential profiles were measured using a zeta-potential/particle-size measurement device (Otsuka Electronics Co., Ltd, ELSZ-2). A solid sample was suspended in distilled water, ethanol (99.5%, Kanto Chemical Co., Inc.), and acetone (99.0%, Kanto Chemical Co., Inc.). The pH of the suspension was adjusted using a 1M NaOH or HCl solution. The dispersion stability of samples in various solvents was determined by a sedimentation experiment. A typical procedure was used to prepare the suspension; first, 15 mg of TiO₂ was mixed with 15 mL solvents and sonicated for 1 h.

2.4 Photocatalytic activity measurements

The UV–Vis absorption spectra of samples were recorded on a Hitachi U-3900H spectrophotometer with an integrating sphere assembly. The photocatalytic activity of samples was evaluated using the photocatalytic decomposition of methylene blue (MB, C₁₆H₁₈N₃S) [23]. Samples (5 mg) were dispersed in a methylene blue (1 × 10⁻⁵ mol/L)

aqueous solution (50 mL). Three milliliters of test liquid was taken from this solution and fed into a quartz cell. The test solution was irradiated at 365 nm by an ultraviolet lamp (Spectroline Spectronics, 4W), and the absorbance at 665 nm, which is the maximum absorption wavelength of methylene blue, was measured using a UV–Vis spectrometer (U-3900H). The decomposition rate of methylene blue containing samples was evaluated from the absorbance obtained with irradiation times.

3. RESULTS and DISCUSSION

3.1 Characterization of samples

Sample names, reaction conditions, total surface area (BET), and fluorine contents (x) in $\text{TiO}_{2-x}\text{F}_{2x}$ are summarized in Table 1, in which, fluorinated TiO_2 (F- TiO_2) samples prepared at various reaction conditions with F_2 gas were named as the F1- TiO_2 , F2- TiO_2 , F3- TiO_2 , and F4- TiO_2 , respectively. The fluorine contents in surface region of F- TiO_2 particles were evaluated from the XPS data. Fluorination temperature and F_2 pressure were increased to enhance the fluorine contents (x) in $\text{TiO}_{2-x}\text{F}_{2x}$. At a temperature higher than 200°C , x became 1.10, which suggests the formation of TiOF_2 . The relative surface area of the samples was determined by the BET method. The BET surface areas of fluorinated TiO_2 samples were in the range of $56.4\text{--}61.3\text{ m}^2/\text{g}$, which are obviously higher than that of untreated TiO_2 ($54.6\text{ m}^2/\text{g}$).

Table 1. Reaction conditions of TiO_2 particles treated with F_2 gas and the fluorine contents (x) in $\text{TiO}_{2-x}\text{F}_{2x}$.

Sample name	Temperature ($^\circ\text{C}$)	F_2 pressure (kPa)	Time (h)	Total surface area (BET, m^2/g)	x in $\text{TiO}_{2-x}\text{F}_{2x}$ ^a
TiO_2	–	–	–	54.6	0.00
F1- TiO_2	25	1.3	1	56.4	0.13
F2- TiO_2	25	6.7	1	61.3	0.18
F3- TiO_2	25	50.5	1	57.2	0.44
F4- TiO_2	200	50.5	1	55.9	1.10

^a Fluorine contents (x) in $\text{TiO}_{2-x}\text{F}_{2x}$ were evaluated from XPS results shown in Fig. 3.

The effects of reaction temperature and F_2 pressure on the TiO_2 crystal structure are shown in Fig. 1 (A). Only a single phase of anatase TiO_2 was observed when fluorination was performed at room temperature (25°C). Fluorination did not cause any shift in the peak position of the TiO_2 phase. This is easily understood because the ionic radius of the fluorine atom (0.133 nm) is nearly the same as that of the replaced oxygen atom (0.132 nm) [16]. However, as shown in Fig. 1 (B), the peak intensity ratio of (101)/(200) shown in Fig. 1 (A) decreased when fluorine pressure increased to 5.5 kPa. This indicates that the crystallinity of TiO_2 gradually decreased by the fluorine substitution. After the fluorination temperature was increased from 25°C to 200°C , some

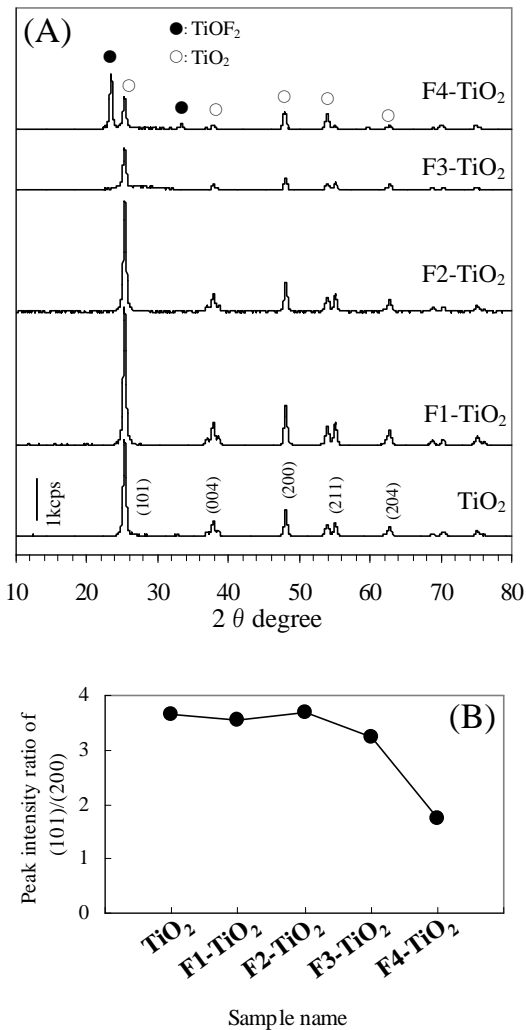


Fig. 1. XRD patterns (A) and peak intensity ratio (B) of (101)/(200) in XRD patterns of untreated TiO₂ and fluorinated TiO₂ (F-TiO₂) particles.

energies were calibrated to the C 1s peak at 284.8 eV of carbon. An F 1s peak located at the binding energy (BE) of 684.3 eV was observed in all F-TiO₂ samples, as shown in Fig. 3 (A). However, the peak at 684.3 eV disappeared after Ar⁺ ions etching, as shown in Fig. 3 (B). Because the fluorine at 684.3 eV is assigned to fluorine atoms chemically adsorbed on TiO₂ surface, they can be easily eliminated by low-energy argon etching (300 V, 5 s). Moreover, an asymmetrical F 1s peak was observed for F3-TiO₂ and F4-TiO₂ samples, where a tailing peak could be found. This means that various chemical forms of F atoms might exist in the samples. Therefore, the F 1s peaks of F3-TiO₂ and F4-TiO₂ samples were deconvoluted into two separated peaks with Gaussian distributions, as shown in Fig. 3 (A). The peak located at 685.2 eV was attributed to the F atom in TiOF₂ [17]. This is easily understood in case of F4-TiO₂ because an obvious TiOF₂ phase appeared in the XRD patterns, as shown in Fig. 1. The peak located at 687.2 eV may be attributed to substituted fluorine atoms in TiO_{2-x}F_{2x} [24]. In the case of Ti 2p (C), the Ti (IV) 2p_{1/2} and Ti (IV) 2p_{3/2} spin-orbital splitting

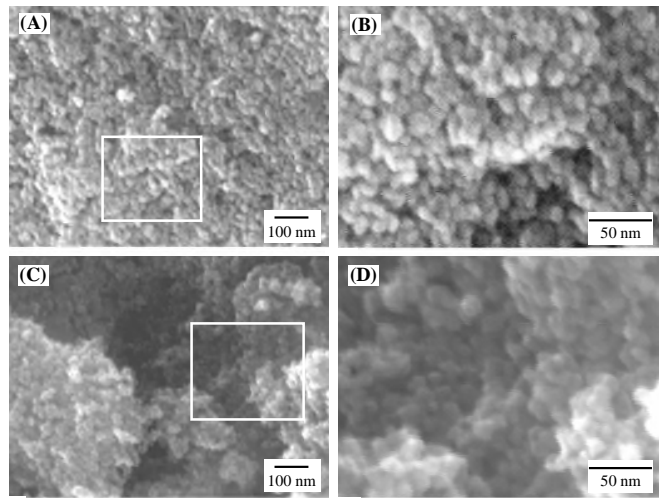


Fig. 2. SEM images of untreated TiO₂ [(A) and (B)] and fluorinated TiO₂ (F4-TiO₂) [(C) and (D)] particles

peaks (●) assigned to TiOF₂ appeared for F4-TiO₂ (TiO_{2-x}F_{2x}, x = 1.10). SEM images of untreated and fluorinated TiO₂ samples are presented in Fig. 2. As seen from Fig. 2 (A) and (C), obvious agglomerates composed of TiO₂ particles with an approximate size of 20 nm were found in all samples. The fluorination effect on the surface morphology of TiO₂ particles could not be detected in the SEM images. However, XPS data confirm the existence of fluorinated surface layer of TiO₂ particles as shown in Fig. 3.

Fig. 3 shows F 1s (A and B), Ti 2p (C), and O 1s (D) spectra of untreated and fluorinated TiO₂ samples. All binding

photoelectrons of the original TiO_2 were located at binding energies of 464.9 eV and 458.9 eV, respectively. However, in the XPS spectrum after fluorination at 25°C , the peak of $\text{Ti } 2p_{3/2}$ shifted to an energy lower than that of original TiO_2 . This result showed that the valence state of Ti^{4+} (458.9 eV) gradually changed to Ti^{3+} (457.0 eV) with increasing F_2 pressure. In the case of F3-TiO_2 , a $\text{Ti } 2p_{3/2}$ peak due to Ti^{2+} (455.2 eV) is especially evident in Fig. 3 (C). Furthermore, when the reaction temperature was increased from 25°C to 200°C , the $\text{Ti } 2p_{3/2}$ peak of F4-TiO_2 shifted to high energy with the creation of Ti-F bond (461.2 eV) of TiOF_2 . Fig. 3 (D) shows the peaks of various samples found at 530.6 eV. The peak intensity decreased with increasing of F_2 pressure. In case of F4-TiO_2 , similar in the $\text{F } 1s$ and $\text{Ti } 2p$ peaks, the $\text{O } 1s$ peak shifted to higher energy. This result seems to be related to the formation of TiOF_2 , as indicated in Fig. 1.

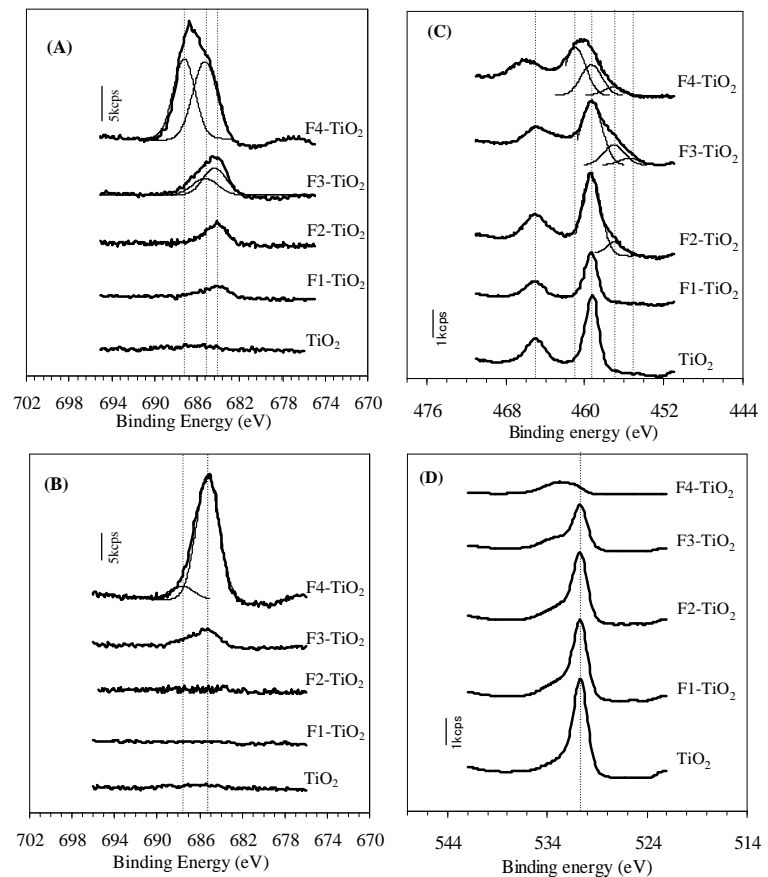


Fig. 3. XPS spectra of $\text{F } 1s$ (A), $\text{F } 1s$ after Ar^+ ion etching (B), $\text{Ti } 2p$ (C), and $\text{O } 1s$ (D) for untreated TiO_2 and fluorinated TiO_2 ($\text{F1-TiO}_2 \sim \text{F4-TiO}_2$) particles.

3.2 Dispersion stability of samples

Fig. 4 shows the suspension of samples dispersed in water (A), and ethanol (B) as polar protic solvents and acetone (C) as a polar aprotic solvent over retention times. In the untreated TiO_2 suspension (a), TiO_2 particles reformed into large agglomerates within 4 h in all solvents. Especially in ethanol (24.3) and acetone (20.7), decreased turbidity in the untreated TiO_2 suspension (a) was observed within 1 h. The dielectric constant of a substance is closely related to the dipole moment. Also, the polarity of a substance with a high dielectric constant is considered to be large. The dispersion stability of

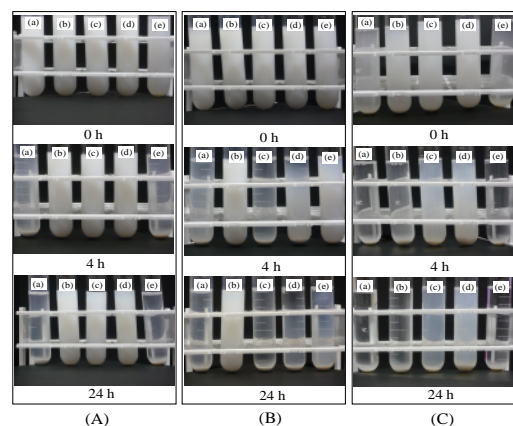


Fig. 4. Suspension of the dispersed samples in water (A), ethanol (B), and acetone (C) with retention times. [(a) TiO_2 , (b) F1-TiO_2 , (c) F2-TiO_2 , (d) F3-TiO_2 , (e) F4-TiO_2]

fluorinated TiO₂ could be sustained in all solvents for 24 h. The stability of colloidal suspensions is primarily governed by interparticle (or surface) forces, especially by the repulsive electrostatic interaction of these charges. Because fluorine at TiO₂ surface has high electronegativity and high acidity, it changes the OH at TiO₂ surface to O⁻ by releasing H⁺ and/or the fluorine (F) changes into the fluoride ion (F⁻) by taking the electron (e⁻) from the O⁻. That is, the surface of F-TiO₂ particles becomes negatively charged and enhances the repulsive interaction between F-TiO₂ particles, as shown later in Fig. 6. Consequently, surface fluorination can alter the particle-particle interactions. However, the formation of TiOF₂ (e) in TiO₂ particles could adversely affect the dispersion stability in all solvents, as shown in Fig. 4.

Fig. 5 depicts the effects of surface fluorination on the particle size (A) and zeta potential (B) of TiO₂ particles in water (■), ethanol (◆), and acetone (▲) at a constant pH of 6.5. The average size and zeta potentials of TiO₂ particles fluorinated at 25°C in all solvents were approximately 11 times smaller and 1.5 times larger, respectively, than those (2.5 × 10³ nm and -19 mV) of untreated TiO₂ particles. Therefore, it can be said that the fluorinated particles can be stabilized against agglomeration by electrostatic forces because the charges increased by surface fluorination are able to create electrostatic repulsion between the particles. However, the dispersion stability of TiO₂ samples (e) fluorinated at 200°C decreased owing to the formation of TiOF₂ film at the particle surface. To improve the dispersion stability of TiO₂ particles, it is important to control the surface fluorination to maintain the state of fluorine adsorbed or partly bonded on the TiO₂ surface without TiOF₂ formation because the high electronegativity and high acidity of fluorine increase the repulsive interactions between TiO₂ particles that is related to dispersion stability in solvents.

3.3 Photocatalytic activity of samples

Surface fluorination obviously affects the UV-Vis absorption characteristics of TiO₂, as shown in Fig. 6. The absorption spectra of the fluorinated TiO₂ samples showed a stronger absorption in the UV-Vis range and a red shift in the band gap transition than untreated TiO₂. This is probably because surface fluorination can expand the wavelength response range of TiO₂ to the visible region. For example, the wavelength range of F3-TiO₂ samples containing Ti³⁺ and Ti²⁺ valences, as shown in Fig. 3 (C), could expand to approximately the 500 nm range owing to a downshift of the conduction band edge. However, in the case of F4-TiO₂ samples, the wavelength range became narrower than that of F3-TiO₂, as indicated in Fig. 6. Also the decrease of surface area

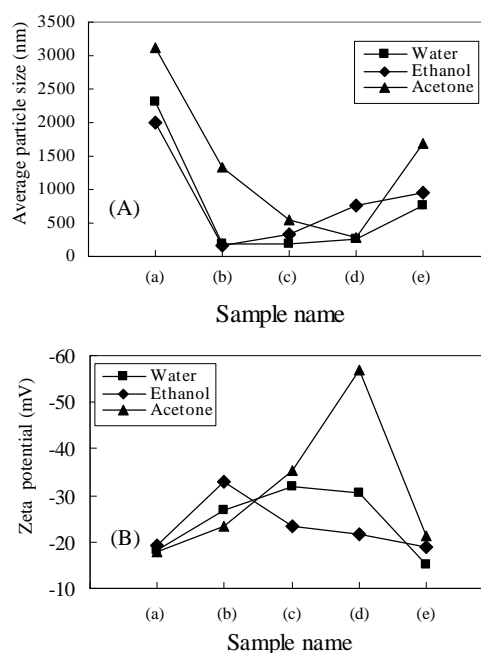


Fig. 5. Average particle size (A) and zeta potential (B) of untreated and fluorinated TiO₂ particles in various solvents (at pH 6.5). [(a) TiO₂, (b) F1-TiO₂, (c) F2-TiO₂, (d) F3-TiO₂, (e) F4-TiO₂]

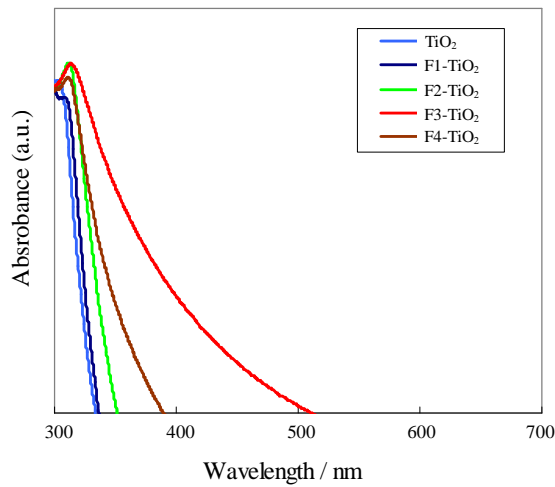


Fig. 6. UV-Vis absorption spectra of various samples.

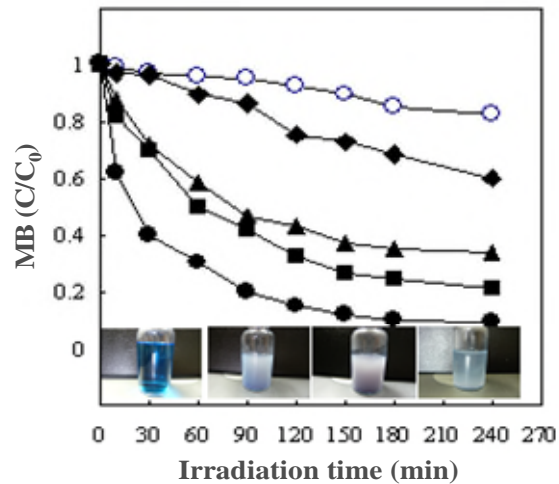
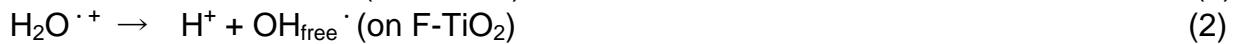


Fig. 8. Photocatalytic degradation of methylene blue (MB) with various samples under UV irradiation. [○; TiO₂, ◆; F1-TiO₂, ▲; F2-TiO₂, ●; F3-TiO₂, ■; F4-TiO₂]

(Table 1)

caused by the TiOF₂ formation may seriously affect the wavelength response range. To compare the photocatalytic activity of untreated and fluorinated TiO₂, the MB degradation reaction was performed and the results are shown in Fig. 7. The MB degradation ratio (73%) with fluorinated TiO₂ was much higher than that (18%) with untreated TiO₂ (○) at 4 h. As suggested by Yang [25], a large number of holes created in fluorinated TiO₂ (F-TiO₂) yields many hydroxyl radicals:



The preferential formation of free OH radicals on F-TiO₂ should subsequently oxidize the MB molecules and the adsorbed amount of MB near the surface will increase simultaneously. Consequently, the photocatalytic activity is enhanced by surface fluorination. In particular, the photocatalytic activity of the F3-TiO₂ sample (●) was superior to other samples because the Ti³⁺ and Ti²⁺ conduction band edges in F3-TiO₂ can trap the photogenerated electrons and lead to the reduction of the recombination rate between excited electrons and holes.

4. CONCLUSIONS

We have reported the effects of surface fluorination on the dispersion stability and photocatalytic activity of TiO₂ particles. Fluorinated TiO₂ (F-TiO₂) was successfully prepared by direct fluorination using F₂ gas. The fluorine contents (x) in TiO_{2-x}F_{2x} were primarily dependent on the reaction temperature and fluorine pressure. At room temperature (25°C) and fluorine pressure lower than 6.7 kPa, the fluorine contents (x) were controlled below 0.18, and the fluorine was chemically adsorbed on the TiO₂

surface. At 200°C, the fluorine content (x) in $\text{TiO}_{2-x}\text{F}_{2x}$ increased to 1.10 and the existence of TiOF_2 was confirmed. The chemically adsorbed fluorine on the TiO_2 surface might play a positive role both toward the dispersion stability and photocatalysis. Especially for the photocatalytic activity of TiO_2 , F3- TiO_2 with Ti^{3+} and Ti^{2+} valences could expand to approximately 500 nm of the UV-Vis range, and the photocatalytic activity of F3- TiO_2 was also 4 times higher than the MB degradation ratio (18%) of untreated TiO_2 . However, the dispersion stability and photocatalysis of F4- TiO_2 prepared at 200°C was negatively affected by the formation of TiOF_2 . Therefore, considering the dispersion stability and photocatalytic activity of TiO_2 , it is essential to control the fluorine contents (x), $0 < x < 0.5$ in $\text{TiO}_{2-x}\text{F}_{2x}$ to optimize the beneficial effects of surface fluorination.

REFERENCES

- [1] K.P.S. Parmar, E. Ramasamy, J.W. Lee, J.S. Lee (2010), "A simple method for producing mesoporous anatase TiO_2 nanocrystals with elevated photovoltaic performance", *Scripta Materialia*, **62**, 223–227.
- [2] M. Fujihira, Y. Satoh, T. Osa (1981), "Heterogeneous photocatalytic oxidation of aromatic compounds on TiO_2 ", *Nature*, **293**, 206.
- [3] P.A.M. Hotsenpiller, J.D. Bolt, W. E. Farneth, J.B. Lowekamp, G.S. Rohrer (1998), "Orientation dependence of photochemical reactions on TiO_2 surfaces", *J. Phys. Chem. B*, **102**, 3216–3226.
- [4] R.A. French, A.R. Jacobson, B. Kim, S.L. Isley, R. Lee Penn, P.C. Baveye (2009), "Influence of ionic strength, pH, and cation valence on aggregation kinetics of titanium dioxide nanoparticles", *Environ. Sci. Technol.*, **43**, 1354–1359.
- [5] C.C. Li, S.J. Chang, M.Y. Tai (2010), "Surface chemistry and dispersion property of TiO_2 nanoparticles", *J. Am. Ceram. Soc.* **93**, 4008–4010.
- [6] G. Li, L. Lv, H. Fan, J. Ma, Y. Li, Y. Wan, X.S. Zhao (2010), "Effect of the agglomeration of TiO_2 nanoparticles on their photocatalytic performance in the aqueous phase", *J. Colloid Interface Sci.*, **348**, 342–347.
- [7] Z.M. Yaremko, N.H. Tkachenko, C. Bellmann (2006), "Redispergation of TiO_2 particles in aqueous solutions", *J. Colloid Interface Sci.*, **296**, 565–571.
- [8] N.G. Hoogeveen, M.A.C. Stuart, G.J. Fleer (1996), "Polyelectrolyte adsorption on oxides. 1. Kinetics and adsorbed amounts", *J. Colloid Interface Sci.*, **182**, 133–145.
- [9] M. Iijima, M. Kobayakawa, H. Kamiya (2009), "Tuning the stability of TiO_2 nanoparticles in various solvents by mixed silane alkoxides", *J. Colloid Interface Sci.*, **337**, 61–65.
- [10] J. Shibata, K. Fuji, K. Horai, H. Yamamoto, Kagaku Kogaku Ronbunshu 27 (2001) 497–501.
- [11] J. Shibata, K. Fuji, K. Horai, H. Yamamoto, Kagaku Kogaku Ronbunshu 28 (2002) 641–646.
- [12] A. Vijayabalan, K. Selvam, R. Velmurugan, M. Swaminathan (2009), "Photocatalytic activity of surface fluorinated TiO_2 -P25 in the degradation of Reactive Orange 4", *J. Hazard. Mater.*, **172**, 914–921.

- [13] A. Hattori, M. Yamamoto, H. Tada, S. Ito (1998), "Formation of $\text{TiO}_{2-x}\text{F}_x$ compounds in fluorine-implanted TiO_2 ", *Chem. Lett.*, **27**, 707–708.
- [14] A. Hattori, K. Shimoda, H. Tada, S. Ito (1999), "Photoreactivity of sol-gel TiO_2 films formed on sodalime glass substrates: effect of SiO_2 underlayer containing fluorine", *Langmuir*, **15**, 5422–5425.
- [15] H. Park, W. Choi (2004), "Effects of TiO_2 surface fluorination on photocatalytic reactions and photoelectrochemical behaviors", *J. Phys. Chem. B*, **108**, 4086–4093.
- [16] D. Li, H. Haneda, S. Hishita, N. Ohashi, N. K. Labhsetwar (2005), "Fluorine-doped TiO_2 powders prepared by spray pyrolysis and their improved photocatalytic activity for decomposition of gas-phase acetaldehyde", *J. Fluorine Chem.*, **126**, 69–77.
- [17] D. Li, H. Haneda, N. K. Labhsetwar, S. Hishita, N. Ohashi (2005), "Visible-light-driven photocatalysis on fluorine-doped TiO_2 powders by the creation of surface oxygen vacancies", *Chem. Phys. Lett.*, **401**, 579–584.
- [18] D. Li, N. Ohashi, S. Hishita, T. Kolodiazhnyi, H. Haneda (2005), "Origin of visible-light-driven photocatalysis: A comparative study on H/F doped and N-F-codoped TiO_2 powders by means of experimental characterizations and theoretical calculations", *J. Solid State Chem.*, **178**, 3293–3302.
- [19] J. Yu, J. C. Yu, M. K.-P. Leung (2003), "Effects of acidic and basic hydrolysis catalysts on the photocatalytic activity and microstructures of bimodal mesoporous titania", *J. Catal.*, **217**, 69–78.
- [20] J.H. Kim, H. Sato, T. Kubo, S. Yonezawa, M. Takashima (2011), "Improved Dispersion Stability of Surface-fluorinated TiO_2 Particles", *Chem. Lett.*, **40**, 230–232.
- [21] M. Takashima, Y. Nosaka, T. Unishi (1992), "Reaction between Rare Earth Oxides and Elementary Fluorine on the rare earth oxides and elementary fluorine. I. Fluorination of neodymium oxide", *Eur. J. Solid State Inorg. Chem.*, **29**, 691–703.
- [22] J.H. Kim, H. Umeda, M. Ohe, S. Yonezawa, M. Takashima (2011), "Preparation of Pure LiPF_6 Using Fluorine Gas at Room Temperature", *Chem. Lett.*, **40**, 360–361.
- [23] T. Ohno, T. Tsubota, K. Nishijima, Z. Miyamoto (2004), "Degradation of methylene blue on carbonate species-doped TiO_2 photocatalysts under visible light", *Chem. Lett.*, **33**, 750–751.
- [24] J.C. Yu, J. Yu, W. Ho, Z. Jiang, L. Zhang (2002), "Effects of F-doping on the photocatalytic activity and microstructures of nanocrystalline TiO_2 powders", *Chem. Mater.*, **14**, 3808–3816.
- [25] S.Y. Yang, Y.Y. Chen, J.G. Zheng, Y.J. Cui (2007), "Enhanced photocatalytic activity of TiO_2 by surface fluorination in degradation of organic cationic compound", *J. Environ. Sci.*, **19**, 86–89.